

## Research Article

# Optimization on Material Removal Rate and Surface Roughness of Stainless Steel 304 Wire Cut EDM by Response Surface Methodology

Sathishkumar Seshaiyah,<sup>1</sup> Deepak Sampathkumar <sup>1,2</sup> Mathanbabu Mariappan <sup>1</sup>,  
Ashokkumar Mohankumar <sup>1</sup> Guruprasad Balachandran <sup>3</sup> Murugan Kaliyamoorthy,<sup>4</sup>  
Barathiraja Rajendran <sup>1</sup> and Rajendiran Gopal <sup>5</sup>

<sup>1</sup>Department of Mechanical Engineering, Government College of Engineering, Bargur, Krishnagiri 635 104, Tamil Nadu, India

<sup>2</sup>Department of Mechanical and Automation Engineering, Agni College of Technology, Thalambur, Chennai 600 130, Tamil Nadu, India

<sup>3</sup>Department of Mechanical Engineering, Alagappa Chettiar Government College of Engineering and Technology, Karaikudi 630 003, India

<sup>4</sup>Department of Mechanical Engineering, Government Polytechnic College, Thiruvarur 612 804, India

<sup>5</sup>Department of Motor Vehicle Engineering, Defence University College of Engineering, Bishoftu, Ethiopia

Correspondence should be addressed to Deepak Sampathkumar; [deepak.mae@act.edu.in](mailto:deepak.mae@act.edu.in) and Rajendiran Gopal; [razaautoirtt@gmail.com](mailto:razaautoirtt@gmail.com)

Received 2 May 2022; Accepted 29 July 2022; Published 29 August 2022

Academic Editor: Vijayananth Kavimani

Copyright © 2022 Sathishkumar Seshaiyah et al. This is an open access article distributed under the Creative Commons Attribution License, which permits unrestricted use, distribution, and reproduction in any medium, provided the original work is properly cited.

In this work, wire cut electrical discharge machining (WEDM) is used for the material removing processes; it is utilized for machining conductive parts where it is required to produce complicated shapes, new profiles, new geometry, new product development, and high-accuracy components. This machining process is best suitable for high-end applications such as aerospace, automations, automobile, and medical devices. At present, most of the industrial sectors choose the WEDM process because it is used to develop products in a very short development cycle and at a better economic rate. In this paper, the selected complex geometry of the metal sample was eroded away from the wire during the WEDM process, which eliminates mechanical tensions during machining. The effect of different WEDM operation variables set as wire speed, wire tension, discharge current, dielectric flow rate, and pulse on and off time on the parameter, stainless steel 304 material removing rate (MRR) using RSM, has been studied. The MRR will be maximized if the optimum sets of operational variations are used and also achieve a superior surface finish.

## 1. Introduction

WEDM, also called as “spark,” is a machining technique that employs electrical output to obtain a variety of shapes. WEDM is a unique variation of the traditional EDM technique that starts the electrical sparking process using an electrode. The thin continuous brass, copper, or tungsten made wire electrode with a diameter of 0.05-0.3 mm moves constantly, which makes use of that may attain a better tiny

corner radius of WEDM. Using a series of rapidly recurring current outputs among the two electrodes separated by a dielectric solution and placed at an electric voltage, the material is removed from the workpiece. The tool-electrode, or simply the “tool” or “electrode,” is one of the electrodes, whilst the workpiece-electrode [1, 2], or just the “workpiece”, is the other electrode.

As the distance between the electrodes decreases, the intensity of the electric field in the volume between them

exceeds the strength of the [3–5] dielectric (at least at few point(s), that breakup the allowed current to flow among the two electrodes). This is analogous to the breaking of the capacitor. From this, the material is removed from the two electrodes [6].

When the current flow slows (or stops—based on the generator), fresh solution-based dielectric is frequently introduced into the internal-electrode volume, allowing solid elements to be removed and the dielectric's insulating characteristics to be recovered [7]. Flushing is the process of replenishing the interelectrode volume with a new liquid dielectric. Additionally, following a current flow, the potential differentiation among the two electrodes [8] is recovered to its prebreakdown state, allowing for another liquid dielectric breakdown. Wire EDM is used in various manufacturing industrial applications: soft armors shaping, hybrid composite, and mainly in the coating industries (thermal spray processes) for cutting the base materials into the desired shape [9–20].

The mechanism of wire EDM process parameters is most similar to conventional EDM. The conventional EDM process will create an erosion effect on the sample surfaces to remove the material. The basic mechanism involved in the electric discharge machining (EDM) process is that the tool electrode is the cathode and the sample material is the anode. The developed voltage is passed between the two electrodes, and dielectric medium is passed between them to create a strong electrostatic effect. This effect produces a spark gap between the tool and sample. Huge thermal energy is created, and it melts material and vaporizes the material from the sample. The modification of pulse energy and current durations in the dielectric medium can determine the dimensional accuracy and quality of the machining samples [21–25].

To improve the dimensional accuracy and quality of the wire EDM process, it has many working parameters: surface roughness, metal removal rate, wire feed rate, pulse on time, pulse off time, peak current, pulse current, applied voltage, etc.

These all parameters mostly influence the performance of wire EDM machining processes. The proper selection of optimal parameters plays a very important role in the wire EDM machining process; it leads to dimensional accuracy and a quality surface finish. The improper selection of process parameters will lead to dimensional inaccuracy, poor quality, and surface finish; it also leads to wire breakage in the continued machining process; and it affects the performance of the process [26–29].

The most accurate optimization technique is the response surface methodology (RSM) based linear regression model is used in this work. The popularity and simplicity of this technique needed to control various parameters in the wire EDM process. In the present work, surface roughness, MRR, pulse on time, pulse off time, and peak current values are chosen for performance measurement. The selected parameters are the most essential things to get dimensional accuracy and quality finishing in the WEDM process. Many researchers have proved that using the RSM technique is most helpful in carrying out

experiments with this technique, which leads to minimal experimental effort [30–33].

## 2. Experimentation

**2.1. 304 Grade Stainless Steel.** The most popular stainless steel is SAE 304, commonly known as A2 stainless steel (A2 steel tool not to be confused) with or stainless steel (18/8), standard 1.4301. The major noniron components of steel are chromium (typically 18%) and nickel (usually 8%). Its steel is made of austenite. It is nonmagnetic and not particularly electrically or thermally conductive. It is extensively used because it is easy to mold into different forms and has a better corrosion resistance than ordinary steel. Screws, machinery components, textiles, and other household and industrial items are made of stainless steel 304. These SS 304 grade materials are also used in defense applications like aircraft, armors, and shields as well. But the machining operations performed with this material are very difficult in traditional methods, and there are many proven literature studies available [34–37]. The experiment runs in the WEDM process with various optimized parameter values fed into the machine, and the machined sample design is shown in Figure 1.

**2.2. Stainless Steel: Grade 304 (Uns S30400).** Standard chemical formula: Fe, <0.08% C, 17.5–20% Cr, 8–11% Ni, <2% Mn, <1% Si, <0.045% P, and <0.03% S. Detailed chemical compositions are shown in Table 1.

**2.3. Tool for Machining.** The experiment findings were achieved using an Electronica Machine Tools Ltd wire-cut EDM machine (ULTRACUT S2), as shown in Figure 2. The technical specifications of the ULTRACUT S2 WEDM are shown in Table 2.

**2.4. Performance Measures.** WEDM performance is often assessed using the following criteria, independent of the electrode material and dielectric fluid used.

**2.4.1. Material Removal Rate (MRR).** Its greatest is a key indicator of the WEDM process' efficiency and cost-effectiveness. However, increasing MRR is not necessarily desired for all applications, since it may compromise the work piece's surface integrity. Fast removal rates result in a rough surface finish.

The expression of material removal rate (MRR) can be obtained from the WEDM.  $MRR = \text{cutting velocity} \times \text{wire diameter} \times \text{material thickness}$ .

**2.4.2. Roughness of the Surface ( $R_a$ ).** The WEDM process creates a huge number of craters on the surface, which are created by the discharge energy. The quality of the surface is mostly determined by the amount of energy per spark.

**2.5. Parts Programming in Machine.** The component programming system receives the profile's geometry and the mobility of the wire electrode cutter along its

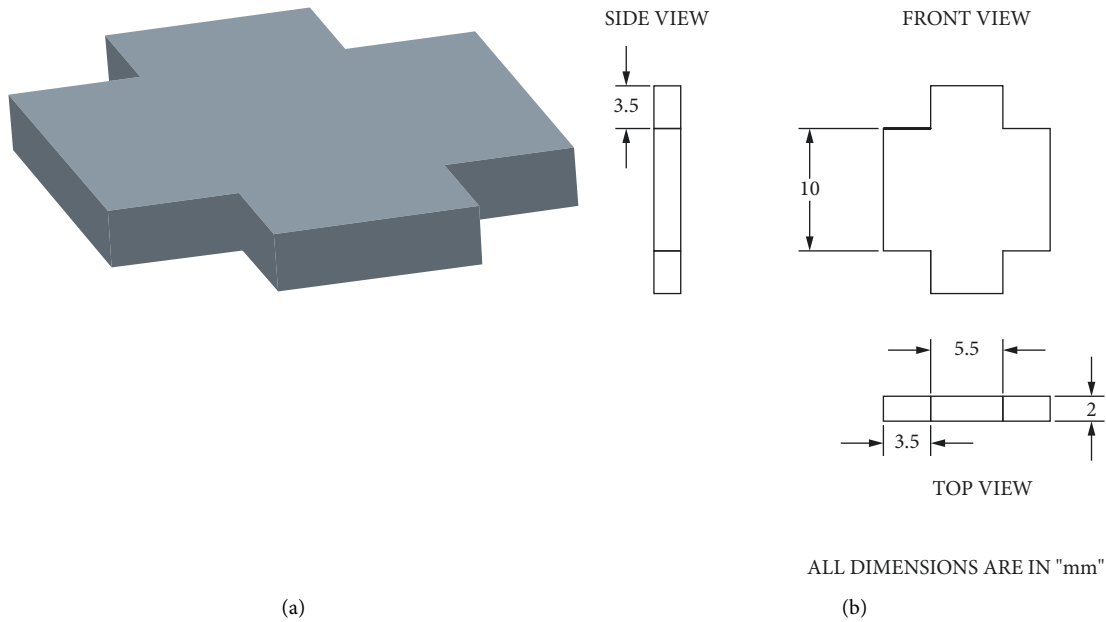


FIGURE 1: (a) Component 3D model and (b) detail 2D drawing.

TABLE 1: Chemical composition.

C%	0.017
Si%	0.41
Mn%	1.80
Cr%	18.08
Mo%	0.57
Cu%	0.56
Ni%	8.02
Co%	0.113
P%	0.031
S%	0.026
N%	0.087

TABLE 2: Technical specification of the ULTRACUT WEDM.

Model	ULTRACUT S2
Make	Electrica, Pune
Generator	El pulse 50 S
<i>Travel range</i>	
Main table traverse (X, Y)	X 600 mm, Y 400 mm
Auxiliary table traverse (Uv)	U ± 40 mm, V ± 40 mm
Vertical	Z 325 mm
Max. table size	860 × 580 mm
Max. work piece size	1150 × 810 x 300
Max. work piece weight	1000 kg
<i>Feed</i>	
Main table feed rate	900 mm/min
Resolution	0.001 mm
Wire feed rate	0.15 m/min
Max. taper cutting range	±15°/100 mm
<i>Dielectric supply unit</i>	
Dielectric fluid	DM water
Dirty tank	900 ltr
Clean tank	300 ltr
Wire diameter	0.25 mm
Program	El cam V1.14 with hardware
Lock	(USB-3049-2943)



FIGURE 2: Wire-cut EDM machine ULTRACUT S2.

keyboard, in terms of different definitions of points, lines, and circles as tool path elements, in a completely menu-driven, conversational manner. Each path element's wire compensation and taper gradient may be customized

individually. After feeding the profile into the computer, all of the path's numerical information is automatically computed, and a printout is produced. On the visual display panel, the entered profile may be checked. The computer records the successful profile definition, which is subsequently sent into the generator for programmed execution. The machine input data are detailed in Tables 3 and 4.

2.6. *Surface Roughness Tester.* The surface roughness value for specified experimental components is measured using

TABLE 3: Input parameters and their levels.

Factor	A	B	C
Input parameter	Pulse ON, (T-ON)	Pulse OFF, (T-OFF)	Peak current(IP)
Units	µs	µs	Amps
Level 1	105	115	125
Level 2	43	53	63
Level 3	170	190	210

TABLE 4: Response surface methodology design.

Sl. no.	X1 (T -ON)	X2 (T- OFF)	X3 (IP)
1	1	0	0
2	0	1	0
3	0	0	0
4	0	-1	0
5	-1	1	-1
6	0	0	1
7	1	-1	1
8	0	0	-1
9	0	0	0
10	0	0	0
11	0	0	0
12	-1	-1	-1
13	1	1	1
14	-1	0	0
15	1	-1	-1
16	-1	-1	1
17	0	0	0
18	0	0	0
19	1	1	-1
20	0	1	-1

TABLE 5: Taylor Hobson.

Model	Surtronic25
Range	00-300 µm
Evaluation length	2.50 mm–25.0 mm
Cutoff	0.25 mm–2.50 mm

TABLE 6: Result of MRR and surface finish.

Wire diameter (mm)	0.25	Material thickness (mm)	2.052
Sl. no.	Cutting velocity. (mm/min)	MRR (mm <sup>3</sup> /min)	Ra,(µm)
1	7.8	3.933	2.711
2	8.2	4.303	2.939
3	8.9	4.557	2.92
4	9.2	4.507	2.802
5	8.6	4.214	2.919
6	9.4	4.474	3.012
7	8	4.325	2.807
8	9.8	4.716	2.946
9	9.6	4.523	2.922
10	8.3	4.572	2.968
11	8.4	4.567	2.926
12	7.6	4.104	2.848
13	7.9	3.807	3.021
14	8.8	4.209	2.784
15	7.4	3.687	2.352
16	9	4.565	2.894
17	9.1	4.557	2.92
18	8.9	4.572	2.938
19	7.8	4.326	2.915
20	7.2	3.736	2.707

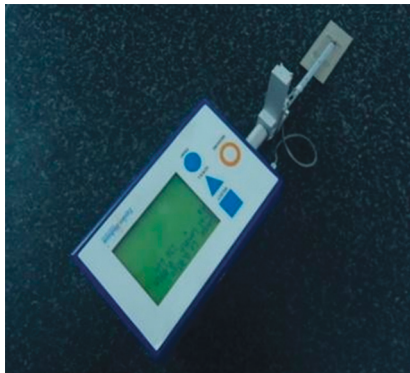


FIGURE 3: Roughness tester.

Taylor Hobson, Surtronic25 Roughness Testers. The surface roughness tester used is presented in Figure 3 and its specifications are listed in Table 5.

2.7. Material Removal Rate: Calculations. The MRR surface finish has conducted 20 experiments with various parameters like cutting velocity, MRR, and surface roughness. Various machining parameters were selected to perform this work. The obtained Ra value of all these experiments is shown in Table 6.

Material Removal Rate (MPR)

$$\begin{aligned}
 &= Vc \times \text{Wire Dia} \times \text{Material Thickness} \\
 &= 7.8 \times 0.25 \times 2.052. \\
 &= 3.933 \frac{\text{mm}^3}{\text{min}}.
 \end{aligned} \tag{1}$$

### 3. Results and Discussions

These experimental results were obtained using a specific WEDM process. The wire diameter is 0.25 mm, the material is brass, and the dielectric fluid is di-ionized water. The experimental design matrix results are displayed in Tables 7–11. The obtained results from experiments are conducted with the specific input process parameters such as pulse on time (T-on),µs; pulse off time (T-off), µs; and peak current(IP), amps, with various levels of experiments shown in Table 7.

From Table 8, it is evaluated that the coefficients of estimated regression for surface roughness are very close to the unity value of (R<sup>2</sup> or R-Sq=0.9860) and the adjusted coefficient is (R<sup>2</sup> or R-Sq Adj.=0.9730). This RSM model indicates the estimators of acceptable values with the proper

TABLE 7: Results obtained from experiment.

Exp. no.	Input process parameter					
	Pulse on time(T-on), $\mu$ s		Pulse off time (T- off), $\mu$ s		Peak current(IP), amps	
	Coded	Actual	Coded	Actual	Coded	Actual
1	1	125	0	53	0	190
2	0	115	1	63	0	190
3	0	115	0	53	0	190
4	0	115	-1	43	0	190
5	-1	105	1	63	-1	170
6	0	115	0	53	1	210
7	1	125	-1	43	1	210
8	0	115	0	53	-1	170
9	0	115	0	53	0	190
10	0	115	0	53	0	190
11	0	115	0	53	0	190
12	-1	105	-1	43	-1	170
13	1	125	1	63	1	210
14	-1	105	0	43	0	190
15	1	125	-1	43	-1	170
16	-1	105	-1	43	1	210
17	0	115	0	53	0	190
18	0	115	0	53	0	190
19	1	125	1	63	-1	170
20	-1	105	1	63	1	210

TABLE 8: Coefficients of estimated regression for surface roughness, Ra.

Term	Coef	SE coef	T	P
Constant	0.682524	2.10589	0.324	0.753
A	0.201951	0.03963	5.096	0.000
B	-0.00411	0.02071	-0.198	0.847
C	-0.099919	0.01431	-6.982	0.000
A * A	-0.001524	0.00017	-9.011	0.000
B * B	-0.000403	0.00016	-2.553	0.029
C * C	0.000184	0.00003	5.286	0.000
A * B	0.001104	0.00008	13.35	0.000
A * C	0.000455	0.00004	10.638	0.000
B * C	-0.00379	0.00004	-8.86	0.000
S		R-Sq		R-Sq (Adj)
0.02419		98.60%		97.30%

TABLE 9: Variance analysis for surface roughness, Ra.

Source	DF	Seq-SS	Adj-SS	Adj-MS	F	P
Regression	9	0.413512	0.413512	0.04592	78.52	0.000
Linear	3	0.109886	0.03622	0.012134	20.63	0.000
Square	3	0.087207	0.10881	0.036395	61.99	0.000
Interactions	3	0.21642	0.21642	0.072064	123.29	0.000
Residual error	10	0.005851	0.005851	0.000573	-	-
Lack of fit	5	0.004096	0.004096	0.000807	2.33	0.187
Pure error	5	0.001755	0.001755	0.00034	-	-
Total	19	0.419363	-	-	-	-

TABLE 10: Coefficients of estimated regression for material removal rate (MRR).

Term	Coef	SE coef	T	P
Constant	-53.3003	6.42397	-8.297	0.000
A	0.986	0.1209	8.155	0.000
B	0.2197	0.06317	3.477	0.006
C	-0.0424	0.04366	-0.971	0.354
A * A	-0.0046	0.00052	-8.963	0.000
B * B	-0.0009	0.00048	-1.901	0.087
C * C	0.0003	0.00011	2.509	0.031
A * B	0.001	0.00025	4.082	0.002
A * C	0.0001	0.00013	0.652	0.529
B * C	-0.0013	0.00013	-10.043	0.000
S		R-Sq		R-Sq(Adj)
0.07379		97.00%		94.40%

TABLE 11: Variance analysis of material removal rate (MRR).

Source	DF	Seq SS	Adj SS	Adj MS	F	P
Regression	9	1.78682	1.78682	0.198536	36.46	0.000
Linear	3	0.09402	0.76464	0.254879	46.81	0.000
Square	3	1.0506	1.09863	0.366211	67.26	0.000
Interactions	3	0.6422	0.6422	0.214067	39.32	0.000
Residual error	10	0.05445	0.05445	0.005445	-	-
Lack of fit	5	0.05275	0.05275	0.010549	31.03	0.001
Pure error	5	0.0017	0.0017	0.00034	-	-
Total	19	1.84127	-	-	-	-

degree of freedom and ideal architecture for reactive extraction process predictive simulations shown in Table 8. The ANOVA predicted results shown in Tables 9–11 give a T-value of 0.324, -8.297; P-value of 0.753; and an F-value of 78.52, 36.46 in the RSM model outlined as significant.

The significance to look at the obtained values in the model is that they correspond to peak current, pulse on time, and pulse off time. The surface roughness values are controlled with pulse on time and pulse off-time set input mean values shown in Tables 8 and 9. The material removal rate will be controlled with peak current modifications shown in Tables 10 and 11. The optimized output responses are shown in Figures 4 to 8.

3.1. Regression Analysis for Material Removal Rate. The findings of the experiments were used to create a mathematical model that expressed the connection between process parameters and MRR. Multiple regressions are used to calculate the coefficients of mathematical models, as shown in Figure 4.

$$\begin{aligned}
 \text{MRR} = & -53.3033 + 0.986 \times \text{Ton} + 0.2197 \times \text{Toff} \\
 & - 0.042 \times \text{IP} - 0.0046 \times \text{Ton}^2 - 0.0009 \times \text{Toff}^2 \\
 & + 0.0003 \times \text{IP}^2 + 0.001 \times \text{Ton} \times \text{Toff} + 0.0001 \\
 & \times \text{Ton} \times \text{IP} - 0.0013 \times \text{Toff} \times \text{IP}.
 \end{aligned} \tag{2}$$

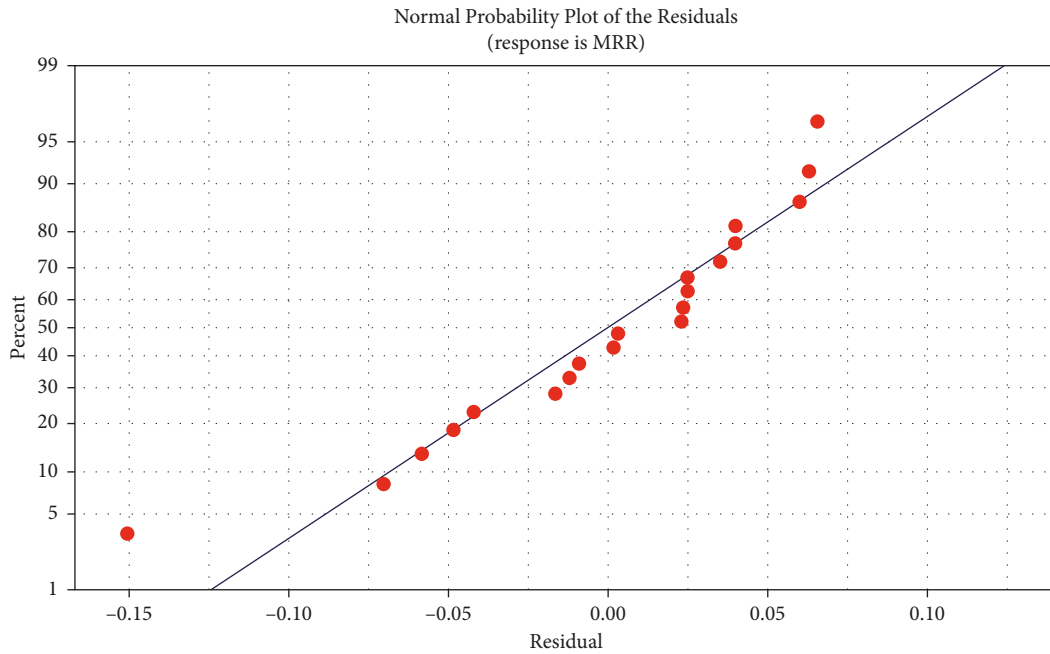


FIGURE 4: Normal probability plot of the residuals of the MRR.

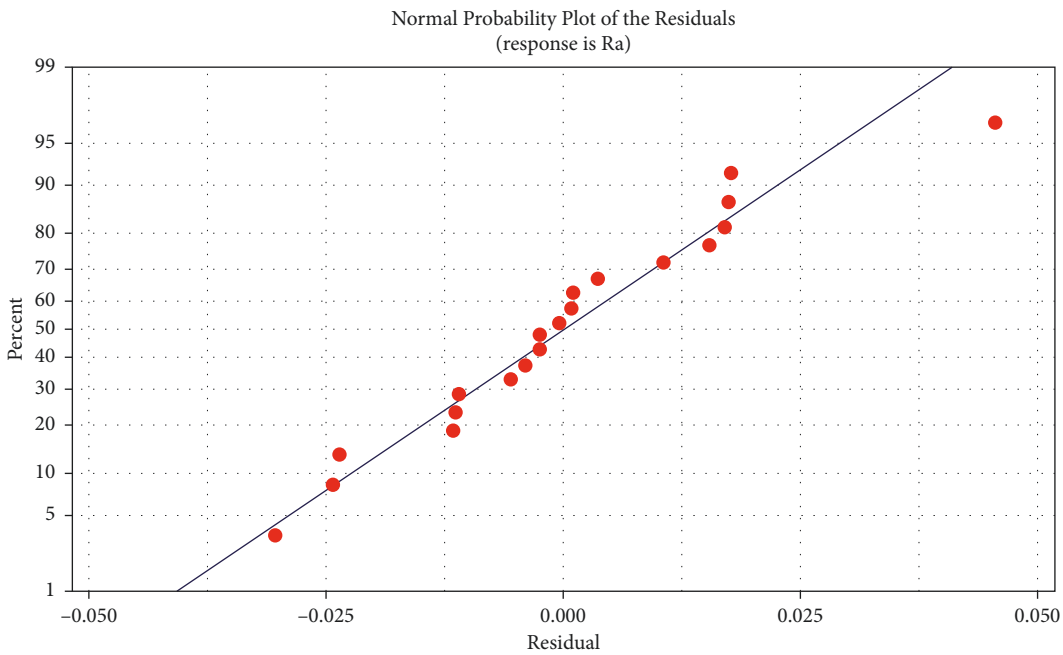


FIGURE 5: Normal probability plot of the residuals of surface roughness. The wire EDM process completed the given input process parameter. Shapes of component profile are shown in Figure 6.

3.2. Regression Analysis for Surface Roughness. The findings of the experiments were utilized to create a mathematical model that expressed the connection between process parameters and surface roughness, as shown in Figure 5. Multiple regressions are used to calculate the coefficients of mathematical models.

$$\begin{aligned}
 SR = & 0.682524 + 0.201951 \times Ton - 0.00411 \times Toff \\
 & - 0.099919 \times IP - 0.001524 \times Ton^2 - 0.000403 \times Toff^2 \\
 & + 0.000184 \times IP^2 + 0.001104 \times Ton \times Toff \\
 & + 0.0004551 \times Ton \times IP - 0.000379 \times Toff \times IP.
 \end{aligned}$$

(3)

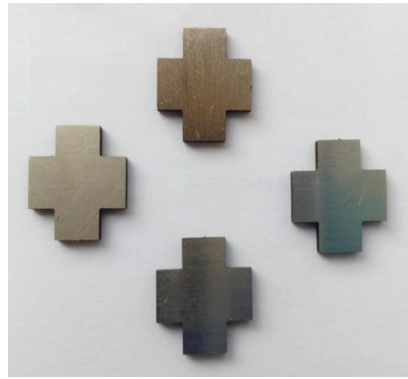


FIGURE 6: Wire EDM component profile.

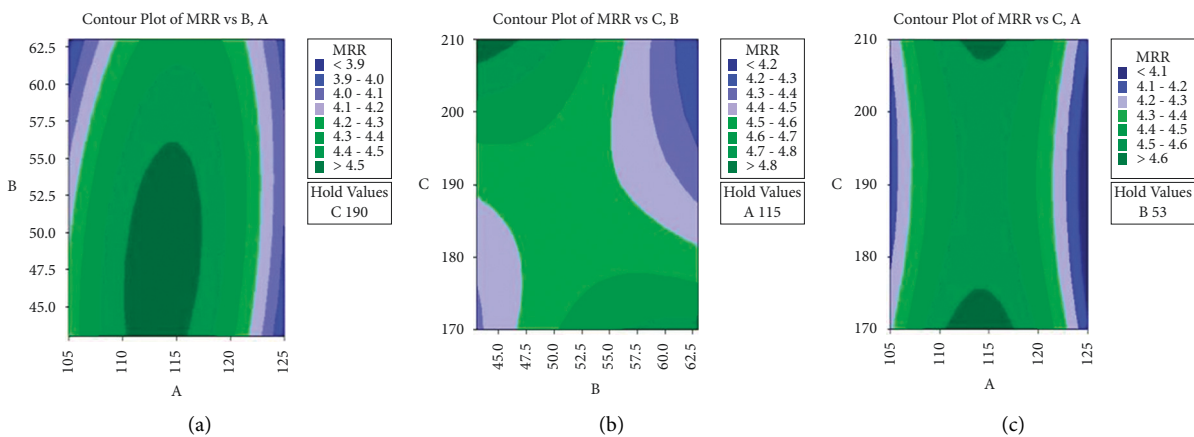


FIGURE 7: (a) Contour plot Of MRR vs (B) A., (b) contour plot of MRR vs (C) B., and (c) contour plot Of MRR vs C, A.

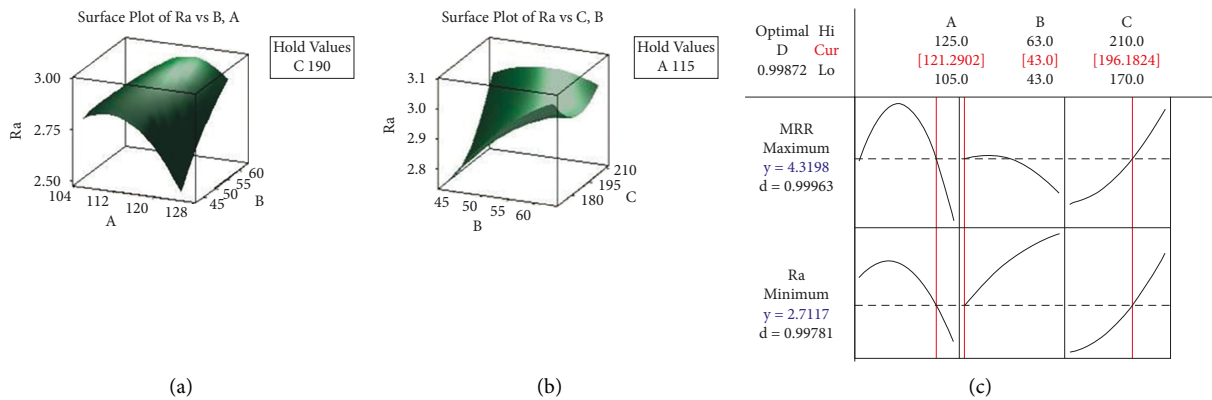


FIGURE 8: (a) Surface plot of Ra vs (C) A., (b) surface plot of Ra vs (C) B., and (c) optimization plot of MRR, Ra.

The response optimization plot for MRR and Ra is shown in Figures 7 and 8. The ultimate goal of our research is to increase MRR while reducing surface roughness.

Figure 7 shows the 2D contour response surface of MRR, and Figure 8 shows the 3D response surface of Ra. The MRR values vary with the changes in the discharge voltage and peak current. The Ra value leads to an electrode spark energy gap between the tool and the sample material. There are many

combinations selected with MRR and Ra parameters, to opt with the graphs. This graph shows the increasing MRR value has a tendency to decrease surface roughness (Ra) [38–42].

In order to evaluate whether the maximum value of MRR and Ra is minimum, the desirability method was utilized to determine the optimal value of variables (Ra). The greatest values of MRR = 4.3198 and Ra = 2.7117 are achieved for the following combination of variables, as shown in the graph [43–45].

$$\begin{aligned}
 T_{\text{On}} &= 121.2902 (\mu\text{s}), \\
 T_{\text{Off}} &= 43 (\mu\text{s}), \\
 IP &= 196.182 (\text{amp}).
 \end{aligned}
 \tag{4}$$

#### 4. Conclusion

- (i) As a consequence, the tests were performed on a WEDM machine, and the experimental research findings were derived from the work completed.
- (ii) The pulse on time increases with respect to the surface roughness.
- (iii) To achieve a superior surface finish for the specified test range in a 304 stainless steel material, utilize a high pulse on time of 121.2902 (s), a low pulse off time of 43.00 (s), and a peak current of 196.182 (amps) in the WEDM Process. The surface roughness optimal value is 2.7117, while the material removal rate is 4.3198.
- (iv) The stainless steel 304 material has better corrosion resistance, high strength in mechanical properties, and is best suited for many chemical industries, automobiles, and customized machine spare manufacturing applications. The hardened stainless steel 304 work materials during re-machining is a major problem in mechanical industries. The wire-cut electric discharge machining process will solve that problem easily.

#### Data Availability

The data used to support the findings of this study are available from the author upon request.

#### Conflicts of Interest

The authors declare that they have no conflicts of interest.

#### Acknowledgments

The authors wish to express their sincere thanks to Dr. S. K. Nayak, Director General, and Dr. K. Prakalathan, Director (Academics), Central Institute of Petrochemicals Engineering and Technology (CIPET), Chennai, Tamil Nadu, India, for the help rendered during characterization, polymer testing lab facilities. The authors also wish to thank Dr. K. P. Bhuvana, Scientist, and R. Joseph Bensingh, Senior Scientist, CIPET: School for Advanced Research in Polymers (SARP)—Advanced Research School for Technology and Product Simulation (ARSTPS), Chennai, Tamil Nadu, India, for their help in carrying out this investigation, and the authors dedicated this work to the Government of India.

#### References

- [1] A. Goswami and J. Kumar, "Investigation of surface integrity, material removal rate and wire wear ratio for WEDM of Nimonic 80A alloy using GRA and Taguchi method," *Engineering Science and Technology, an International Journal*, vol. 17, no. 4, pp. 173–184, 2014.
- [2] F. Kausar, S. Kumar, M. Azam, S. Suman, A. Sharma, and A. Sethi, "Optimization of machining parameter for surface roughness on WEDM of En36 alloy steel," *Journal of Mechanical and Civil Engineering*, vol. 12, no. 6, pp. 101–104, 2015.
- [3] A. Biloria and R. Singh, "Optimizing the parameters influence the performance of wire cut EDM machining," *International Journal of current Engineering and Technology*, vol. 4, no. 5, 2014, <http://inpressco.com/category/ijcet>.
- [4] F. Klocke, D. Welling, A. Klink, D. Veselovac, T. Nöthe, and R. Perez, "Evaluation of advanced wire-EDM capabilities for the manufacture of fir tree slots in Inconel 718," *Procedia CIRP*, vol. 14, pp. 430–435, 2014.
- [5] C. D. Shah, J. R. Mevada, and B. C. Khatri, "Optimization of process parameter of wire electrical discharge machine by response surface methodology on Inconel-600," *International Journal of Emerging Technology and Advanced Engineering*, vol. 3, no. 4, pp. 2250–2459, 2013.
- [6] K. Kumar and R. Ravikumar, "Modeling and optimization of wire EDM process," *International Journal of Modern Engineering Research*, vol. 3, no. 3, pp. 1645–1648, 2013.
- [7] F. Han, J. Jiang, and D. Yu, "Influence of discharge current on machined surfaces by thermo-analysis in finish cut of WEDM," *International Journal of Machine Tools and Manufacture*, vol. 47, no. 7-8, pp. 1187–1196, 2007.
- [8] K. Kanlayasiri and S. Boonmung, "Effects of wire-EDM machining variables on surface roughness of newly developed DC 53 die steel: design of experiments and regression model," *Journal of Materials Processing Technology*, vol. 192-193, pp. 459–464, 2007.
- [9] K. Mathivanan, D. Thirumalaikumarasamy, M. Ashokkumar, S. Deepak, and M. Mathanbabu, "Optimization and prediction of AZ91D stellite-6 coated magnesium alloy using box behnken design and hybrid deep belief network," *Journal of Materials Research and Technology*, vol. 15, pp. 2953–2969, 2021.
- [10] M. Ashokkumar, D. Thirumalaikumarasamy, C. Ramachandran et al., "Enhancing the corrosion resistance of low pressure cold sprayed metal matrix composite coatings on AZ31B Mg alloy through friction stir processing," *Coatings*, vol. 12, no. 2, p. 135, 2022.
- [11] M. Mathanbabu, D. Thirumalaikumarasamy, P. Thirumal, and M. Ashokkumar, "Study on thermal, mechanical, microstructural properties and failure analyses of lanthanum zirconate based thermal barrier coatings: a review," *Materials Today Proceedings*, vol. 46, pp. 7948–7954, 2021.
- [12] M. Ashokkumar, D. Thirumalaikumarasamy, P. Thirumal, and R. Barathiraja, "Influences of Mechanical, Corrosion, erosion and tribological performance of cold sprayed Coatings A review," *Materials Today Proceedings*, vol. 46, pp. 7581–7587, 2021.
- [13] M. Kannan, T. Duraisamy, T. Pattabi, and A. Mohankumar, "Investigate the corrosion properties of stellite coated on AZ91D alloy by plasma spray technique," *Thermal Science*, vol. 26, no. 2, pp. 911–920, 2022.
- [14] S. Deepak, D. Thirumalaikumarasamy, M. Ashokkumar, and S. K. Nayak, "Experimental analyzing the static puncture resistance performance of shear thickening fluid impregnated polypropylene hybrid composite target structures for armour application," *Journal of the Textile Institute*, pp. 1–13, 2022.



- [15] S. Deepak, D. Thirumalaikumarasamy, P. Thirumal, and M. Ashokkumar, "Static puncture resistance characteristics with various indenter nose shape geometry perforation of shear thickening fluid impregnated polypropylene fabric for soft armour application," *Polymers and Polymer Composites*, vol. 30, Article ID 096739112110633, 2022.
- [16] S. Deepak, D. Thirumalaikumarasamy, P. Thirumal et al., "Preparation and characterization of shear thickening fluid coated polypropylene fabric for soft armour application," *Journal of the Textile Institute*, vol. 112, no. 10, pp. 1555–1567, 2021.
- [17] M. Ashokkumar, D. Thirumalaikumarasamy, S. Deepak, and T. Sonar, "Electrochemical corrosion performance of friction stir processed cold spray metal matrix composite coatings on AZ31B magnesium alloy under sodium chloride environment," *Surface Topography: Metrology and Properties*, vol. 10, no. 3, Article ID 035010, 2022.
- [18] Ľ. Straka and S. Hašová, "Optimization of material removal rate and tool wear rate of Cu electrode in die-sinking EDM of tool steel," *International Journal of Advanced Manufacturing Technology*, vol. 97, no. 5-8, pp. 2647–2654, 2018.
- [19] S. Deepak, K. P. Bhuvana, R. J. Bensingh, K. Prakalathan, and S. K. Nayak, "Development of hybrid composites and joining technology for lightweight structures," *Advances in Polymer Sciences and Technology*, pp. 123–131, 2018.
- [20] S. Dinesh, A. G. Antony, K. Rajaguru, and V. Vijayan, "Experimental investigation and optimization of material removal rate and surface roughness in centerless grinding of magnesium alloy using grey relational analysis," *Mechanics and Mechanical Engineering*, vol. 21, no. 1, pp. 17–28, 2017.
- [21] V. Gaikwad and V. S. Jatti, "Optimization of material removal rate during electrical discharge machining of cryo-treated NiTi alloys using Taguchi's method," *Journal of King Saud University - Engineering Sciences*, vol. 30, no. 3, pp. 266–272, 2018.
- [22] P. M. Abhilash and D. Chakradhar, "Wire EDM failure prediction and process control based on sensor fusion and pulse train analysis," *International Journal of Advanced Manufacturing Technology*, vol. 118, no. 5-6, pp. 1453–1467, 2022.
- [23] P. M. Abhilash and D. Chakradhar, "Failure detection and control for wire EDM process using multiple sensors," *CIRP Journal of Manufacturing Science and Technology*, vol. 33, pp. 315–326, 2021.
- [24] K. Rajmohan and A. S. Kumar, "Experimental investigation and prediction of optimum process parameters of micro-wire-cut EDM of 2205 DSS," *International Journal of Advanced Manufacturing Technology*, vol. 93, no. 1-4, pp. 187–201, 2017.
- [25] T. Bergs, U. Tombul, T. Herrig, M. Olivier, A. Klink, and F. Klocke, "Analysis of characteristic process parameters to identify unstable process conditions during wire EDM," *Procedia Manufacturing*, vol. 18, pp. 138–145, 2018.
- [26] T. Muthuramalingam and B. Mohan, "A review on influence of electrical process parameters in EDM process," *Archives of Civil and Mechanical Engineering*, vol. 15, no. 1, pp. 87–94, 2015.
- [27] D. Jafari, T. H. Vaneker, and I. Gibson, "Wire and arc additive manufacturing: opportunities and challenges to control the quality and accuracy of manufactured parts," *Materials & Design*, vol. 202, Article ID 109471, 2021.
- [28] A. Alias, B. Abdullah, and N. M. Abbas, "Influence of machine feed rate in WEDM of titanium Ti-6Al-4V with constant current (6A) using brass wire," *Procedia Engineering*, vol. 41, pp. 1806–1811, 2012.
- [29] K. H. Ho, S. T. Newman, S. Rahimifard, and R. D. Allen, "State of the art in wire electrical discharge machining (WEDM)," *International Journal of Machine Tools and Manufacture*, vol. 44, no. 12-13, pp. 1247–1259, 2004.
- [30] A. Mandal and A. R. Dixit, "State of art in wire electrical discharge machining process and performance," *International Journal of Machining and Machinability of Materials*, vol. 16, no. 1, pp. 1–21, 2014.
- [31] A. Chaudhary, S. Sharma, and A. Verma, "Optimization of WEDM process parameters for machining of heat treated ASSAB '88 tool steel using Response surface methodology (RSM)," *Materials Today Proceedings*, vol. 50, pp. 917–922, 2022.
- [32] B. Choudhuri, R. Sen, S. K. Ghosh, and S. C. Saha, "Modelling and multi-response optimization of wire electric discharge machining parameters using response surface methodology and grey-fuzzy algorithm," *Proceedings of the Institution of Mechanical Engineers - Part B: Journal of Engineering Manufacture*, vol. 231, no. 10, pp. 1760–1774, 2017.
- [33] A. Çiçek, T. Kivak, and E. Ekici, "Optimization of drilling parameters using Taguchi technique and response surface methodology (RSM) in drilling of AISI 304 steel with cryogenically treated HSS drills," *Journal of Intelligent Manufacturing*, vol. 26, no. 2, pp. 295–305, 2015.
- [34] V. N. Gaitonde, M. Manjiaiah, S. Maradi, S. R. Karnik, P. M. Petkar, and J. P. Paulo Davim, "Multiresponse optimization in wire electric discharge machining (WEDM) of HCHCr steel by integrating response surface methodology (RSM) with differential evolution (DE)," *Computational Methods and Production Engineering*, pp. 199–221, Woodhead Publishing, 2017.
- [35] K. Ishfaq, N. Ahmad, M. Jawad, M. A. Ali, and A. Al-Ahmari, "Evaluating material's interaction in wire electrical discharge machining of stainless steel (304) for simultaneous optimization of conflicting responses," *Materials*, vol. 12, no. 12, p. 1940, 2019.
- [36] G. Ugrasen, M. Bhagawan Singh, and H. V. Ravindra, "Optimization of process parameters for SS304 in wire electrical discharge machining using taguchi's technique," *Materials Today Proceedings*, vol. 5, no. 1, pp. 2877–2883, 2018.
- [37] T. Chaudhary, A. N. Siddiquee, and A. K. Chanda, "Effect of wire tension on different output responses during wire electric discharge machining on AISI 304 stainless steel," *Defence Technology*, vol. 15, no. 4, pp. 541–544, 2019.
- [38] M. Ashokkumar, D. Thirumalaikumarasamy, T. Sonar, S. Deepak, P. Vignesh, and M. Anbarasu, "An overview of cold spray coating in additive manufacturing, component repairing and other engineering applications," *Journal of the Mechanical Behavior of Materials*, vol. 31, no. 1, pp. 514–534, 2022.
- [39] P. M. Gopal and K. Soorya Prakash, "Minimization of cutting force, temperature and surface roughness through GRA, TOPSIS and Taguchi techniques in end milling of Mg hybrid MMC," *Measurement*, vol. 116, pp. 178–192, 2018.
- [40] S. Karthik, K. S. Prakash, P. M. Gopal, and S. Jothi, "Influence of materials and machining parameters on WEDM of Al/AlCoCrFeNiMo0.5 MMC," *Materials and Manufacturing Processes*, vol. 34, no. 7, pp. 759–768, 2019.

- [41] P. M. Gopal, K. S. Prakash, and S. Jayaraj, "WEDM of Mg/CRT/BN composites: effect of materials and machining parameters," *Materials and Manufacturing Processes*, vol. 33, no. 1, pp. 77–84, 2018.
- [42] G. R. K. V, G. P.M, and S. D, "Multi-response optimization and surface integrity characteristics of wire electric discharge machining  $\alpha$ -phase Ti-6242 alloy," *Process Integration and Optimization for Sustainability*, vol. 5, no. 4, pp. 815–826, 2021.
- [43] R. Prasanna, P. M. Gopal, M. Uthayakumar, and S. Aravind, "Multicriteria optimization of machining parameters in WEDM of titanium alloy 6242," *Lecture Notes in Mechanical Engineering*, , pp. 65–75, Springer, 2019.
- [44] M. Ashokkumar, D. Thirumalaikumarasamy, S. Deepak et al., "Optimization of cold spray process inputs to minimize porosity and maximize hardness of metal matrix composite coatings on AZ31B magnesium alloy," *Journal of Nanomaterials*, vol. 2022, Article ID 7900150, 17 pages, 2022.
- [45] R. Pradeep Raj, D. Thirumalaikumarasamy, C. Ramachandran et al., "Optimisation of HVOF spray process parameters to achieve minimum porosity and maximum hardness in WC-10Ni-5Cr coatings," *Coatings*, vol. 12, no. 3, p. 339, 2022.